SUPPLEMENTAL INFORMATION TITLES AND LEGENDS

Supplemental information

Document S1. Figures S1-S8 and Table S1

Data S1. Excel file containing data too large to fit in a PDF, related to Figure 3

Data S2. Excel file containing data too large to fit in a PDF, related to Figure 4

Figure S1. Mutagenesis studies of nuclear localization signals (NLSs) and nuclear export signals (NESs) in GFP fused HPIV3-M and NiV-M.

(A) Positively charged amino acid residues in the bipartite NLSs or key leucine residues in the potential NESs were mutated to alanine. (B) HeLa cells expressing either wild-type (WT), NLS mutant (Mbp1/2), or NES mutant (L106A L107A) forms of GFP-fused HPIV3-M and NiV-M were fixed and stained with Hoechst to visualize nuclei. Representative fields of cells expressing each construct are shown. Scale bars represent 20 μm (C) Quantification of the cytoplasmic/nuclear GFP intensity (C: N) ratios for 30–50 individual cells was analyzed for each mutant, as described in the Materials and Methods. Statistical significance was determined by one-way ANOVA with Dunnett's multiple comparison test. **** $P < 0.0001$.

Figure S2. Effects of HPIV3 infection and matrix protein on host translational profile.

(A) Polysome profiles of mock-infected (black), HPIV3 infected (blue), or HPIV3-M transfected (red) HEK-293Ts at 48 hrs post-infection. HEK-293Ts were infected with HPIV3 (MOI of 5) or transfected with matrix for 48 hrs and cytoplasmic extracts were prepared for polysome profiling. Cytoplasmic extracts were sedimented through a 10–50% sucrose gradient and 0.6 ml fractions were collected while continuously measuring absorbance at $\lambda = 254$nm. (B)

Proteins were TCA precipitated from the collected fraction with equal volume and analyzed by immunoblotting to determine the sedimentation of S6, L7a, eIF4AIII, Y14, MAGOH, and HPIV3-M with ribosomal subunits, monosomes, or polysomes. (C-D) Densitometric quantification of the indicated proteins (S6 and L7a) across 16 fractions from (B). The y-axis shows the percentage of the total integrated intensity (% of Total Int) for each protein in the indicated condition: mock infection (black), HPIV3 infection (blue), and HPIV3 matrix protein expression (red).

Figure S3. Nuclear-cytoplasmic trafficking of HPIV3 matrix protein (HPIV3-M) during infection.

(A) HeLa cells infected with HPIV3 at m.o.i of 5 and then incubated with fresh growth medium for up to 24 hrs. At 12, 16, 20, and 24 hours of post-infection, cells were fixed and counterstained with anti-HPIV3-M antibody (red) to label viral matrix protein, and nuclei were stained with Hoechst (blue). Representative fields of cells at each time point are shown. Scale bars represent 20 μm (B) Quantification of cytoplasmic/nuclear HPIV3-M intensity (C: N) ratios was performed on 30–50 individual cells, as described in the Materials and Methods. Statistical significance was analyzed by one-way ANOVA with Dunnett. **** P <0.0001; ns, not significant.

Figure S4. Effects of the exon junction complex on Paramyxovirus infection.

HEK-293T cells were transfected with siRNA pools targeting eIF4A3**,** Y14, MAGOH, or non-targeting control siRNAs (NC), respectively. At 48 hrs post-transfection, cells were inoculated with the designated virus (A) HPIV3, (B) Cedar, (C) MuV, and (D) NDV at a multiplicity of infection (m.o.i.) of 0.01. The number of GFP-positive cells in each well was acquired at the indicated time points by Celigo imaging cytometer (Nexcelom). Relative fold changes (FC) in GFP-positive cells per well were then calculated. Symbols represent the data points from biological triplicates. Bars represent the mean of the triplicates. Statistical significance was determined by two-way ANOVA with Dunnett multiple comparison test. * *P* <0.05; ** *P* <0.01; *** *P* <0.001; **** *P* <0.0001; ns, not significant.

Figure S5. Subcellular localization of eIF4AIII in HeLa cells expressing GFP fused HPIV3 matrixes.

Left panel HeLa cells expressing either wild-type (WT), NLS mutant (Nbp1/2), or NES mutant (L106A L107A) forms of GFP-fused HPIV3-M and NiV-M were fixed and stained with anti-eIF4AIII (red) and Hoechst for nuclei (blue), and GFP fluorescence indicates M expression.

Representative fields of cells for each condition are shown. Scale bars represent 20 μm. Right panel: Quantification of cytoplasmic/nuclear eIF4AIII intensity (C: N) ratios was performed on 30 individual cells, as described in Materials and Methods. Statistical significance was analyzed by one-way ANOVA with Dunnett multiple comparison test. **** *P* <0.0001; ns, not significant.

Figure S6. Effects of HPIV3 infection on NMD activity.

HEK-293T cells infected with HPIV3 at m.o.i of 0.01 and analyzed at 24 and 48 hours of post-infection. Endogenous targets of the NMD mRNA surveillance pathway, SC35, GABARAPL1, ASNS, and CARS were analyzed by quantitative RT-PCR. Relative quantification (Gene/GAPDH) is normalized to uninfected controls. Symbols are data points from biological triplicates. Bar represents the mean ± SD. Statistical significance was determined by one-way ANOVA with Dunnett multiple comparison test. * P <0.05; **** P <0.0001; ns, not significant.

Figure S7. Effects of HPIV3 matrix on NMD activity.

HEK-293T cells were transfected with the indicated protein and analyzed at 24 and 48 hrs post-transfection. Endogenous targets of the NMD mRNA surveillance pathway, SC35, GABARAPL1, ASNS, and CARS were analyzed by quantitative RT-PCR. Relative quantification (Gene/GAPDH) is normalized to uninfected controls. Symbols are data points from biological triplicates. Bar represents the mean ± SD. Statistical significance was determined by two-way ANOVA with Bonferroni's multiple comparisons test. ns, not significant.

Figure S8. Recovery of rHPIV3ΔM-mCherry and rHPIV3ΔM viruses in BSR-T7 cells.

Representative images from the rescue of (A) rHPIV3ΔM-mCherry and (B) rHPIV3ΔM at day 3 of post-transfection in BSR-T7 cells. Images were captured by EVOS m5000.

Table S1: qPCR primers, related to Star Methods.

Data S1: Mapped viral read counts of polysome profile mRNA sequencing for HPIV3-WT and HPIV3-delta-M virus.

Tab 1: TPM normalized viral genes expression for HPIV3-WT and HPIV3-delta-M virus.

Tab 2: Ribosome association efficiency of viral transcripts for HPIV3-WT and HPIV3-delta-M virus.

Data S2. Mapped read count of polysome profile mRNA sequencing for Mock, HPIV3-WT and HPIV3-delta-M samples.

Figure S1.

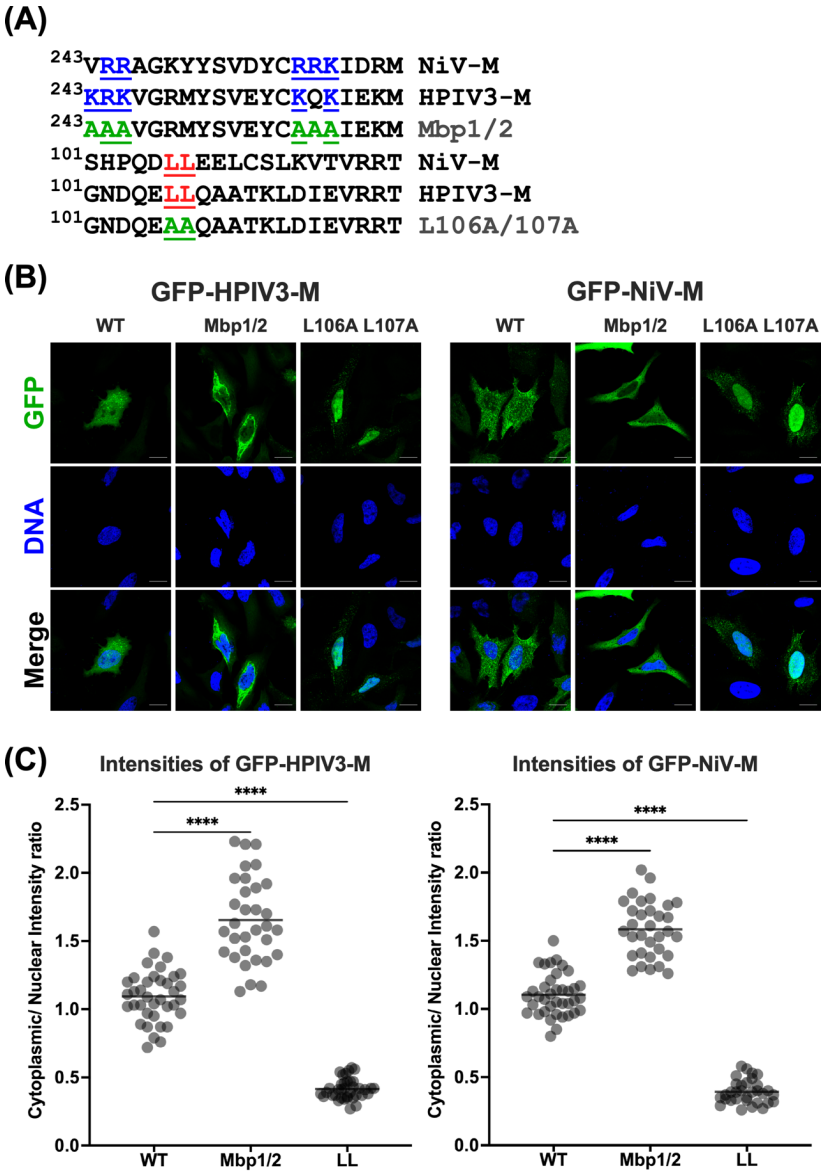

Figure S1. Mutagenesis studies of nuclear localization signals (NLSs) and nuclear export signals (NESs) in GFP fused HPIV3-M and NiV-M. (A) Positively charged amino acid residues in the bipartite NLSs or key leucine residues in the potential NESs were mutated to alanine. (B) HeLa cells expressing either wild-type (WT), NLS mutant (Mbp1/2), or NES mutant (L106A L107A) forms of GFP-fused HPIV3-M and NiV-M were fixed and stained with Hoechst to visualize nuclei. Representative fields of cells expressing each construct are shown. Scale bars represent 20 μm (C) Quantification of the cytoplasmic/nuclear GFP intensity (C: N) ratios for 30–50 individual cells was analyzed for each mutant, as described in the Materials and Methods. Statistical significance was determined by one-way ANOVA with Dunnett's multiple comparison test. **** $P < 0.0001$.

Figure S2.

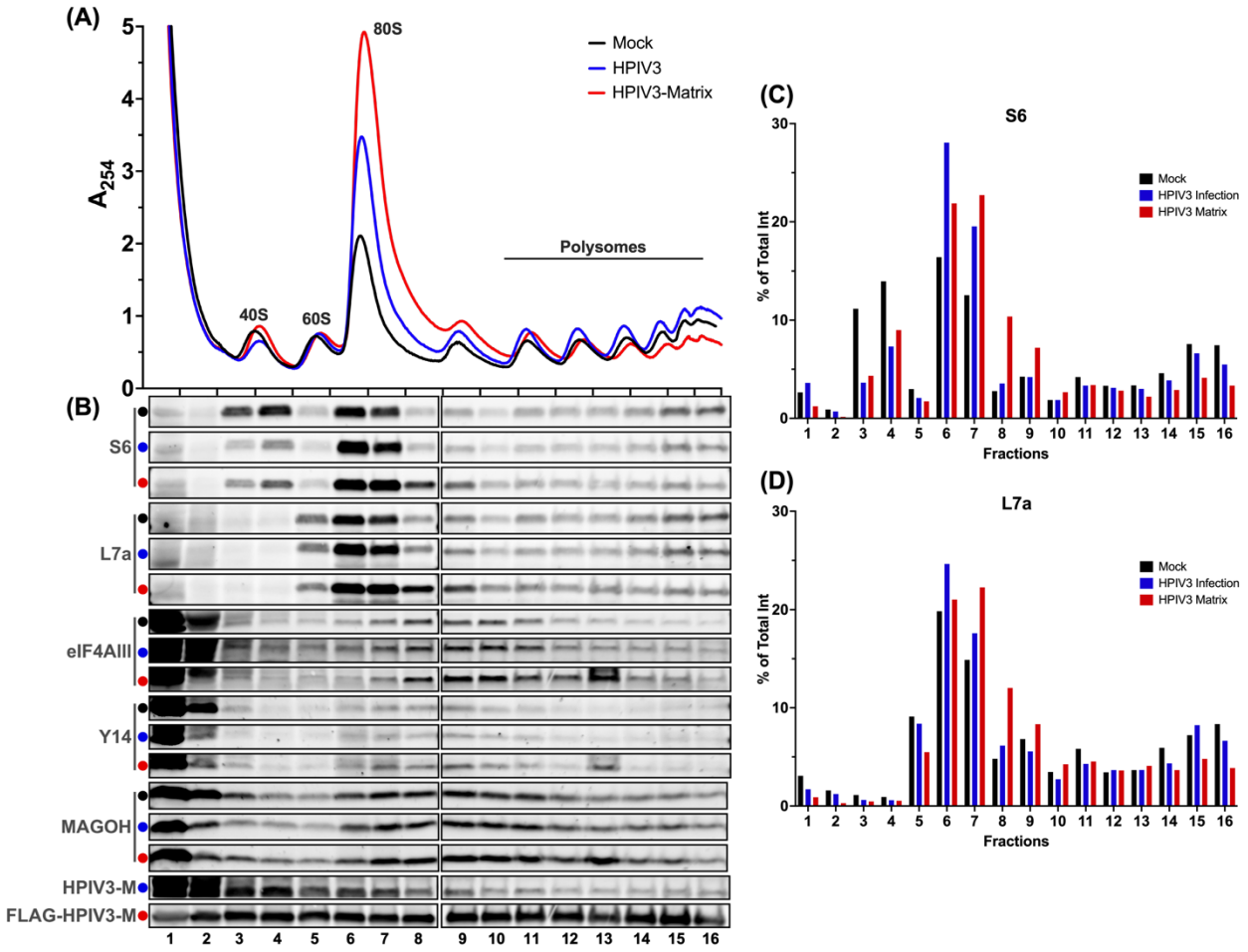

Figure S2. Effects of HPIV3 infection and matrix protein on host translational profile. (A) Polysome profiles of mock-infected (black), HPIV3 infected (blue), or HPIV3-M transfected (red) HEK-293Ts at 48 hrs post-infection. HEK-293Ts were infected with HPIV3 (MOI of 5) or transfected with matrix for 48 hrs and cytoplasmic extracts were prepared for polysome profiling. Cytoplasmic extracts were sedimented through a 10–50% sucrose gradient and 0.6 ml fractions were collected while continuously measuring absorbance at λ = 254nm. (B) Proteins were TCA precipitated from the collected fraction with equal volume and analyzed by immunoblotting to determine the sedimentation of S6, L7a, eIF4AIII, Y14, MAGOH, and HPIV3-M with ribosomal subunits, monosomes, or polysomes. (C-D) Densitometric quantification of the indicated proteins (S6 and L7a) across 16 fractions from (B). The y-axis shows the percentage of the total integrated intensity (% of Total Int) for each protein in the indicated condition: mock infection (black), HPIV3 infection (blue), and HPIV3 matrix protein expression (red).

Figure S3.

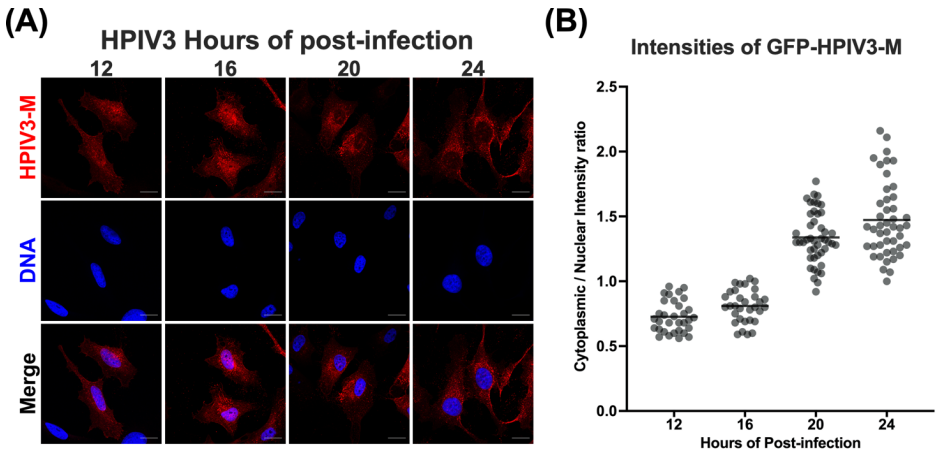

Figure S3. Nuclear-cytoplasmic trafficking of HPIV3 matrix protein (HPIV3-M) during infection. (A) HeLa cells infected with HPIV3 at m.o.i of 5 and then incubated with fresh growth medium for up to 24 hrs. At 12, 16, 20, and 24 hours of post-infection, cells were fixed and counterstained with anti-HPIV3-M antibody (red) to label viral matrix protein, and nuclei were stained with Hoechst (blue). Representative fields of cells at each time point are shown. Scale bars represent 20 μm (B) Quantification of cytoplasmic/nuclear HPIV3-M intensity (C: N) ratios was performed on 30–50 individual cells, as described in the Materials and Methods. Statistical significance was analyzed by one-way ANOVA with Dunnett. **** P <0.0001; ns, not significant.

Figure S4.

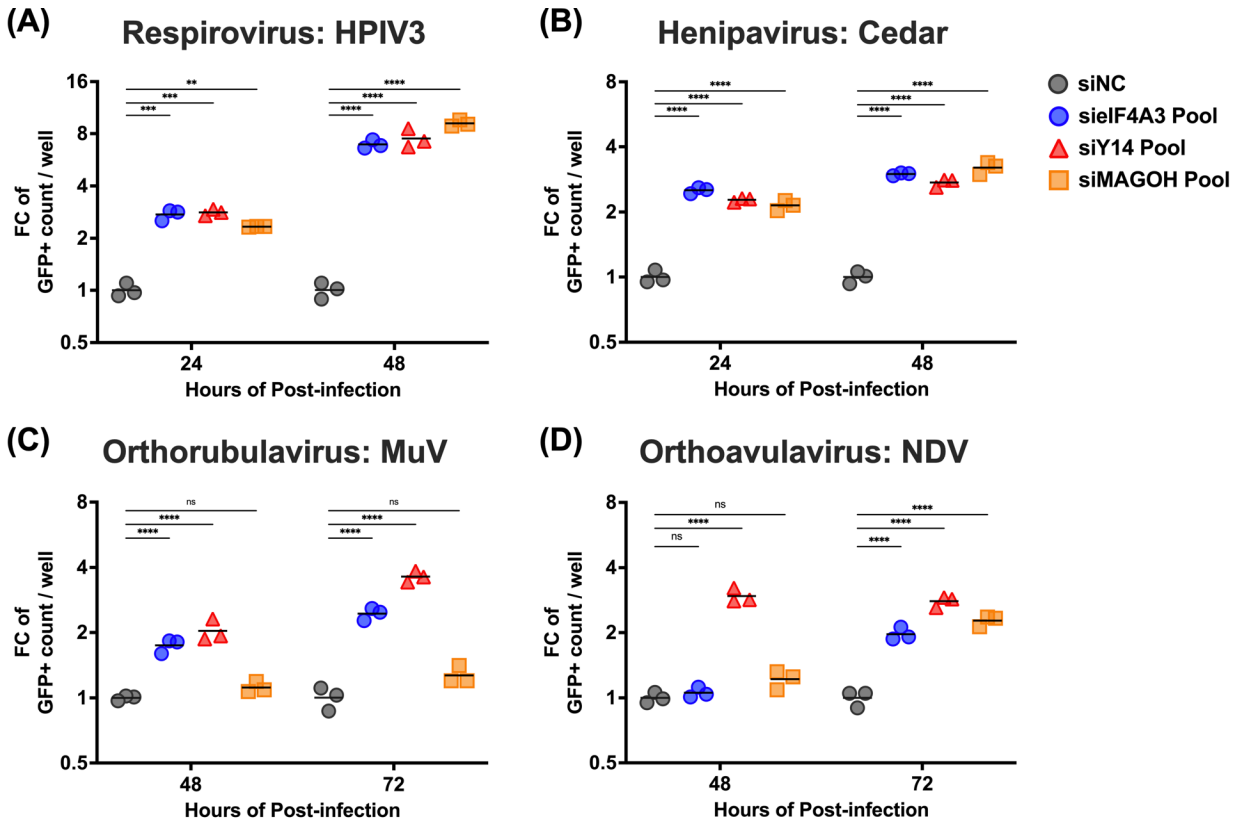

Figure S4. Effects of the exon junction complex on Paramyxovirus infection. HEK-293T cells were transfected with siRNA pools targeting eIF4A3**,** Y14, MAGOH, or non-targeting control siRNAs (NC), respectively. At 48 hrs post-transfection, cells were inoculated with the designated virus (A) HPIV3, (B) Cedar, (C) MuV, and (D) NDV at a multiplicity of infection (m.o.i.) of 0.01. The number of GFP-positive cells in each well was acquired at the indicated time points by Celigo imaging cytometer (Nexcelom). Relative fold changes (FC) in GFP-positive cells per well were then calculated. Symbols represent the data points from biological triplicates. Bars represent the mean of the triplicates. Statistical significance was determined by two-way ANOVA with Dunnett multiple comparison test. * P <0.05; ** P <0.01; *** P <0.001; **** P <0.0001; ns, not significant.

Figure S5.

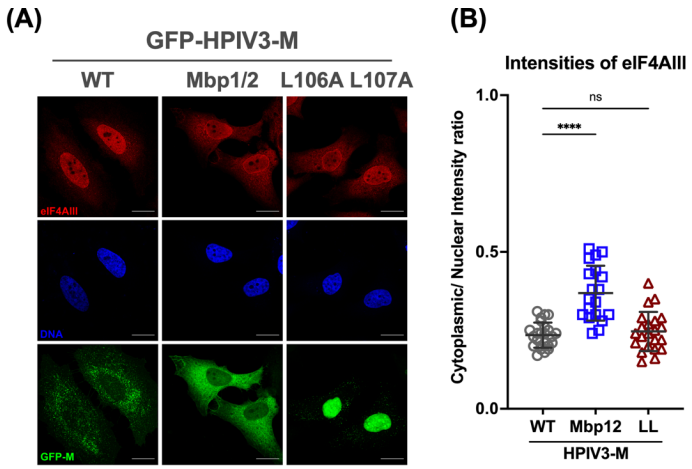

Figure S5. Subcellular localization of eIF4AIII in HeLa cells expressing GFP fused HPIV3 matrixes. Left panel HeLa cells expressing either wild-type (WT), NLS mutant (Nbp1/2), or NES mutant (L106A L107A) forms of GFP-fused HPIV3-M and NiV-M were fixed and stained with anti-eIF4AIII (red) and Hoechst for nuclei (blue), and GFP fluorescence indicates M expression. Representative fields of cells for each condition are shown. Scale bars represent 20 μm. Right panel: Quantification of cytoplasmic/nuclear eIF4AIII intensity (C: N) ratios was performed on 30 individual cells, as described in Materials and Methods. Statistical significance was analyzed by one-way ANOVA with Dunnett multiple comparison test. **** *P* <0.0001; ns, not significant.

Figure S6.

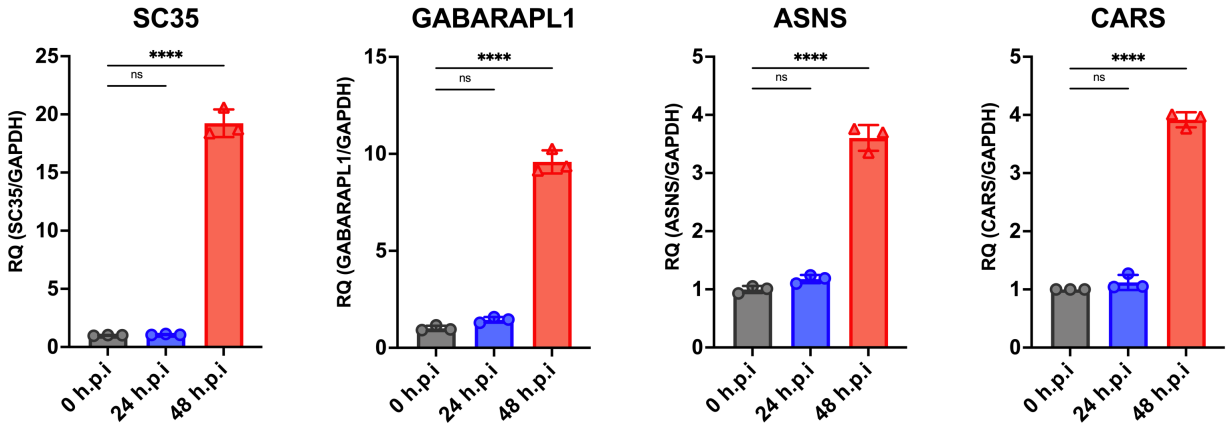

Figure S6. Effects of HPIV3 infection on NMD activity. HEK-293T cells infected with HPIV3 at m.o.i of 0.01 and analyzed at 24 and 48 hours of post-infection. Endogenous targets of the NMD mRNA surveillance pathway, SC35, GABARAPL1, ASNS, and CARS were analyzed by quantitative RT-PCR. Relative quantification (Gene/GAPDH) is normalized to uninfected controls. Symbols are data points from biological triplicates. Bar represents the mean ± SD. Statistical significance was determined by one-way ANOVA with Dunnett multiple comparison test. * P <0.05; **** P <0.0001; ns, not significant.

Figure S7.

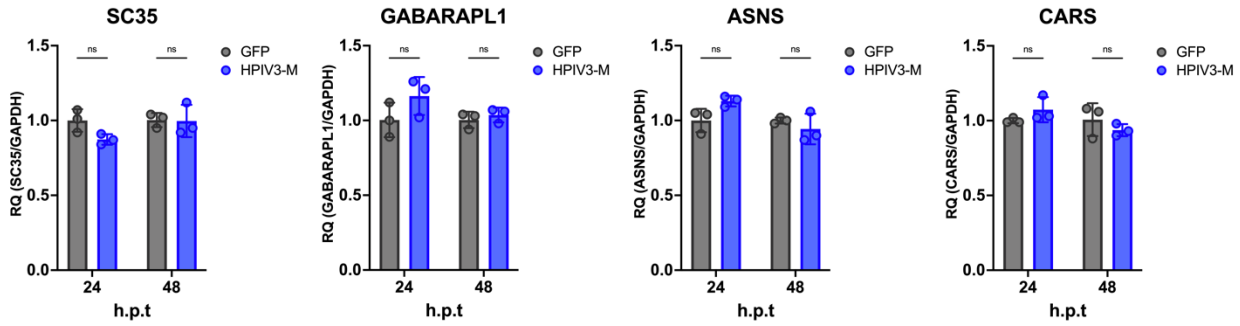

Figure S7. Effects of HPIV3 matrix on NMD activity. HEK-293T cells were transfected with the indicated protein and analyzed at 24 and 48 hrs post-transfection. Endogenous targets of the NMD mRNA surveillance pathway, SC35, GABARAPL1, ASNS, and CARS were analyzed by quantitative RT-PCR. Relative quantification (Gene/GAPDH) is normalized to uninfected controls. Symbols are data points from biological triplicates. Bar represents the mean ± SD. Statistical significance was determined by two-way ANOVA with Bonferroni's multiple comparisons test. ns, not significant.

Figure S8.

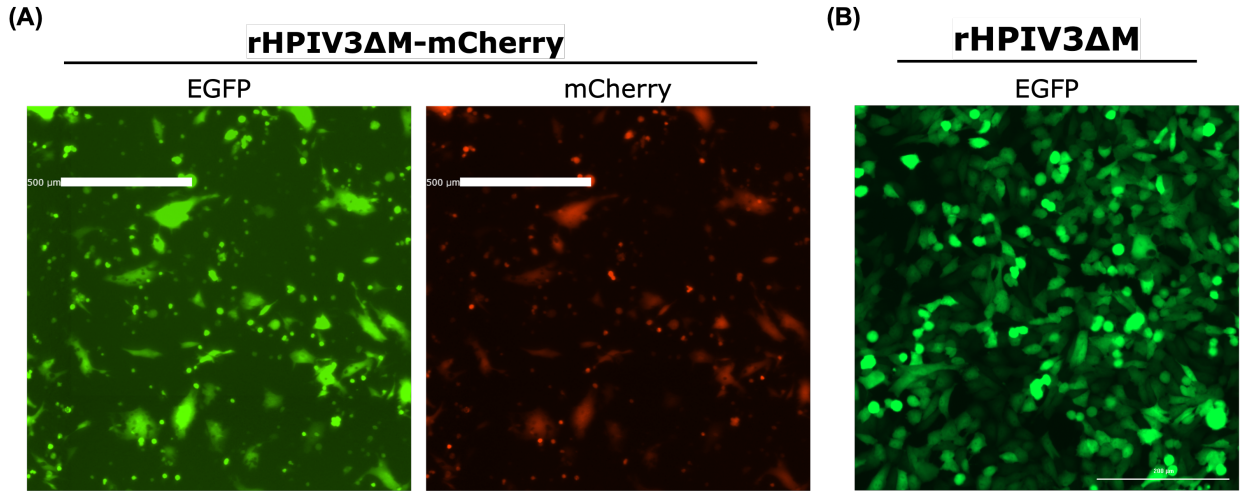

Figure S8. Recovery of rHPIV3ΔM-mCherry and rHPIV3ΔM viruses in BSR-T7 cells. Representative images from the rescue of (A) rHPIV3ΔM-mCherry and (B) rHPIV3ΔM at day 3 of post-transfection in BSR-T7 cells. Images were captured by EVOS m5000.

Table S1.

Table S1: qPCR primers, related to Star Methods.

Gene	Forward Primer (5' to 3')	Reverse Primer (5' to 3')
SC35	CGGTGTCCTCTTAAGAAAATGATGTA	CTGCTACACAACTGCGCCT
ASNS	GGAAGACAGCCCCGATTTACT	AGCACGAACTGTTGTAATGTCA
CARS	CCATGCAGACTCCACCTTTAC	GCAATACCACGTCACCTTTTTC
GABARAPL1	GGCCAGTTCTACTTCTTAATCCGG	AGGTGCTCCCATCTGCTGGG
NiV_N	CGTGGTTATCTTGAGCCTATGT	TCCCAGTCTATTTGCCATGTT
NiV_P	GGAGCATCGAGAGGTCAATAAG	GGACTTTGGCATCGGAGTT
NiV_L	GCGTCTCAGAGGGTAAACATAG	GAGTACACTCCCTGCAAACTTA
NiV_Genome	TCTCCCAGAGTCTATCAGTAAGG	TCCCAGTCTATTTGCCATGTT
NiV_Antigenome	AACTTAGGAACCAAGACAAACAC	CTAGCCGCCTCTTCAAAGATA
18S	GTAACCCGTTGAACCCCATT	CCATCCAATCGGTAGTAGCG
GAPDH	CCACATCGCTCAGACACCAT	AAAAGCAGCCCTGGTGACC
Luciferase	GATCCTCAACGTGCAAAAGAAGC	TCACGAAGGTGTACATGCTTTGG